Environmental Science Nano

Accepted Manuscript

ROYAL SOCIETY OF CHEMISTRY

rsc.li/es-nano

Sublethal doses of ZnO nanoparticles remodel production of cell signaling metabolites in the root colonizer *Pseudomonas chlororaphis* O6.

Jordan Goodman[1,3], Joan E. Mclean[2], David W. Britt[3] and Anne J Anderson[1]

1 Department of Biology, Utah State University, Logan Utah 84322 5305 USA

2 Utah Water Research Laboratory, Utah State University, Logan, Utah 84322 8200 USA

3 Department of Biological Engineering, Utah State University, Logan, Utah 84322 4105 USA

Correspondence

Anne J Anderson

anne.anderson@usu.edu

Cell signaling molecules function in regulating activities both within the producing bacterium as well as between cells. This paper shows that ZnO nanoparticles effectively disrupt cell signaling in a rhizosphere-competent bacterium, *Pseudomonas chlororaphis* O6. The reduced production of phenazines observed with increasing doses of ZnO NPs correlated with lowered levels of the quorum sensing molecules, acylhomoserine lactones (AHSLs). The ZnO NPs had a higher efficacy than Zn ions in these responses. Linked with changes to phenazine production was an effect on Fe metabolism manifest by enhanced siderophore production as Zn concentration from NPs or ions increased. The ZnO NPs induced phenotypes of lowered phenazines, AHSLs and increased siderophores are those observed with a mutant lacking the global regulator GacS. These metabolic changes caused by exposure to ZnO NPs could alter the way in which the bacterium functions in the rhizosphere.

Key words

Phenazines, acylhomoserine lactones, ZnO nanoparticles, siderophore

Nano impact

Purposeful applications of formulations of ZnO nanoparticles as a fertilizer to increase the Zn content of crop plants in soils where Zn is of low bioavailability is feasible. This work addresses the impact of sublethal doses of ZnO nanoparticles on a rhizosphere pseudomonad typical of microbes that have beneficial effects on plants. The work shows shifts in bacterial metabolism through effects on the quorum sensing system such that the role of the microbe in the plants rhizosphere could be altered. The work illustrates the complexity of potential effects of nanoparticles in the environment.

1. Introduction

The unique properties of nanoparticles (NPs) are fundamental in the development of extensive applications for nano-products in commerce. ZnO NPs are used in a wide array of products from sunscreens, to ceramics, to superconductors and opticoelectronic devices.[1-4] An interest in formulations containing ZnO NPs for crop fertilization is developing because of their slow release of the essential metal. [5,6] This paper addresses the bioreactivity of commercially-produced ZnO NPs to a bacterium, *Pseudomonas chlororaphis* O6 (*Pc*O6), that upon root colonization promotes plant performance under both biotic and abiotic stress.[7-10] The changes in metabolism induced by exposure of bacterial cells to ZnO NPs could have commercial applications as well as providing information about impacts of NPs in the environment.

This paper focuses on the mechanism underlying the impact of ZnO NPs on the reduction of phenazine production in *Pc*O6.[11] Phenazines play important roles in the rhizosphere both for the survival of the plant and bacteria. The phenazines have antifungal activity, thus limiting growth of plant pathogenic fungi to aid in plant disease control.[7,12,13] Antagonism of fungal growth is correlated with the induction of reactive oxygen species and chelation of Fe by the phenazines. [14] Their interaction with other microbial factors such as cyclic lipopeptides may enhance inhibition of fungal growth and, thus, disease control;[15] phenazines also stimulate induced resistance in plants.[16] They promote bacterial cell survival when cells are growing in a biofilm[17], in part by acting as an alternative electron acceptor when oxygen is limiting[18] and by conditioning the composition of the extracellular polymeric matrix.[19,20,21] Their regulation of gene expression in the producing bacterium is documented.[19,21] Consequently, understanding factors that control production of phenazines in the plant-associated bacterium is important.

Phenazine production requires the intracellular accumulation to active levels of other signaling molecules, called acyl homoserine lactones (AHSLs). In *P. chlororaphis* 30-84 induction of genes in the phenazine biosynthetic operon is conditioned by 3-OH C6 AHSL with the *phzI* gene encoding a synthase for this structure.[22] Annotation of the *Pc*O6 genome, [23] reveals the genes for phenazine biosynthesis from chorismate to the hydroxyphenazines are clustered between loci PchlO6_5220-5227 with adjacent regulatory genes, *phzR* (PchlO6_5219) and *phzI* (PchlO6_5218).

Exposure of cells to ZnO NPs means that they are responding to both the particles and the ions released from the NP surfaces.[24,25] Our finding of inhibited phenazine production with ZnO NPs counters the observation showing Zn ions (0.5 mg/L) enhance production of phenazine-1-carboxylate (PCA) in *P. fluorescens* 2-79. [26] In another root-colonizing pseudomonad, *P. putida,* reduction in energy status occurs with immediate exposure to 1 mg/L Zn ions in water suspensions of 10^8 cells/ml.[27] Consequently, we compared the metabolic responses of *Pc*O6 between the NPs and Zn ions.

The levels of soluble Zn released from the NPs were determined in the medium, with and without cells, to help to understand the role of the soluble metal in the responses. We used GEOCHEM modeling[28] to estimate the complexation of Zn in the Phz medium and the level of free ions to understand how soluble levels changed with dose of the ZnO NPs. The effect of the Phz medium on NP particle size was evaluated by dynamic light scattering and the association of NPs with the bacterial cell surface was examined by helium ion (HIM) and confocal microscopy.

Thin layer chromatographic separation showed *Pc*O6 to produce the yellow-colored PCA and the orange pigments, 2- hydroxyphenazine and 2- hydroxyphenazine-1-carboxylate (2OH-PCA).[29] In this paper we used liquid chromatographic separation followed by mass spectral

identification[30] to determine whether the composition of the phenazines was changed through effects on the hydroxylation step. Also, we examined the levels of phenazines that were secreted as well as those associated with the cell to determine whether there was an effect of the ZnO NPs on secretion of the phenazines through transporters that may differ between the phenazines structures.[31] To determine whether changes in phenazine production was correlated with changes in AHSLs, these were assayed using a chromogenic assay with *Chromobacterium violaceum*[32] as a biosensor as well as chemically by mass spectral identification.[30] The changes in PVD formation were determined by observing fluorescence after treatment with EDTA to remove chelated metal.[33,34] The EDTA was added to remove metals that could interfere with the fluorescence of PVD. [33,34]

2. Materials and methods

2.1. Source of NPs and characterization

ZnO NPs were purchased from Sigma-Aldrich, MO, USA which indicates a nomimal size of about 50 nm. They have been characterized previously for shape and size by AFM [33.34] and their aggregation in water suspensions by field flow fractionation [27] and by dynamic light scattering analysis.[25] The product is of high purity as demonstrated by the elemental composition.[10,25]

Changes in size of the ZnO NPs in the bacterial growth medium compared to sterile deionized water were analyzed by dynamic light scattering using a DynaPro NanoStar instrument (Wyatt Technology Corporation, Santa Barbara CA) that uses a 658 nm laser and 7.03 Dynamic software package to deduce the hydrodynamic radius of the particles. The data shown are averages of the means obtained from ten 5 sec acquisition times for three separate samples. The ZnO NPs were suspended at 200 mg/L and assayed after 5 h.

2.2. Growth of *Pc*O6 cultures and visualization of cell-NP interactions

*Pc*O6 cultures were maintained as freezer stocks in 15 % glycerol at -80 °C. Inoculum was transferred to growth medium, termed Phz medium, in 50 ml cultures at 28 °C with shaking at 150 rpm in the absence of light for 48 h. The Phz medium contained in 1 L: 15.12 g PIPES, 0.16 g KH_2PO_4, 0.26 g NaCl, 0.50 g $(NH_4)_2SO_4$, 2.58 g glucose, 2.58 g mannitol, 0.64 g $MgSO_4.\cdot 7H_2O$, 140 mg $CaCl_2$, 1.54 mg $MnSO_4\cdot H_2O$, 1.8 mg H_3BO_3, 0.06 mg $CuSO_4$, 1.54 mg $ZnSO_4\cdot 5H_2O$, 1.26 mg $Na_2MoO_4\cdot H_2O$ with adjustment to pH 6.8 with KOH followed by addition of 4 g Proteose Peptone No. 3. This Phz medium was amended with ZnO NPs to provide Zn at 5, 50, and 500 mg/L or with Zn ions from $ZnNO_3$ to added 5, 15, 30 and 90 mg Zn/L or with 5.6 mg/L (100 μM) Fe from $FeCl_3$. These growth studies with the designated NP or ion concentration were repeated three separate times, with each treatment for each experiment being performed in duplicate. Cell populations at harvest were assessed by serial dilution of the cultures onto lysogeny broth (LB) plates and counting colonies after 3 days of growth at 28 °C. Each sample was inoculated in triplicate. For assessment of phenazine accumulation, cells were harvested from the cultures as a pellet through centrifugation at 10,000 g for 10 minutes. Both pellet and the supernatants were retained for analysis.

The association of the bacterial cell surface with the NPs was examined microscopically. Cells were cultured 48 h in Phz medium before transfer to silicon wafers coated with a100 nm oxide layer. HIM was performed with a Carl Zeiss Orion Plus instrument (Peabody, MA. USA) with a beam current of 30.0 Pa and an accelerating voltage of 30 kV. Other samples were examined by confocal microscopy using autofluorescence of cells excited at 405 nm in a Zeiss LSM 710 with the cell suspension being viewed on glass slides. Imaging was performed with a Plan-Apochromat 63x/1.40 oil DIC objective.

2.3. Extraction and characterization of phenazines and AHSLs

Phenazines were extracted from both the culture medium and the cells into acidified ethyl acetate. Equal volumes (15 ml) of solvent and culture supernatant or 10 ml solvent for the cells pelleted from the 50 ml cultures were used.[29] These extracts were dried under air and dissolved in 1 ml ethanol with storage at -20 °C. Absorbance of the ethanol extracts was recorded at 366 nm as a measure of the mixture of phenazines produced by *Pc*O6. The AHSLs were extracted similarly except with nonacidified ethyl acetate. [30,35] The level of secreted AHSLs was detected using the *C. violaceum* detector with 5 µl of the ethanolic solution being added to 1 ml of LB medium containing an inoculum of 10^6 sensor cells. After 1 day growth at 28 °C with shaking at 100 rpm, 1 ml ethanol was added to each culture and the mixture centrifuged at 10,000 g for 10 min. The supernatants were read at 570 nm to assess the formation of violacein dependent on the level of AHSL. Control studies were run to test that the ethanol did not affect growth of the detector strain and that there was linearity in results dependent on dose of the extract.

For identification of specific phenazine or AHSL structures, the ethanol samples were fractionated by an Agilent liquid chromatography system with peaks subjected to mass spectral analysis.[21] Peaks at desired mass corresponding to phenazine and AHSLs structures were identified and quantified as areas under the peak by the Agilent MassHunter software program.

2.4. Determination of soluble metal levels

Soluble metal was assayed in the culture fluids obtained from centrifugation of the cultures, and as a control the noninoculated Phz medium, at 15,500 g for two sequential 30 min periods. The levels of soluble Fe and Zn were determined by inductively coupled plasma mass spectrometry

(ICP-MS) after acid hydrolysis. GEOCHEM modeling[28] was used to determine the speciation of Fe and Zn in the Phz medium based on its composition.

2.5. Determination of siderophore levels

The level of PVD in the 48 h culture supernatants was determined by measuring fluorescence between 460-500 nm with excitation at 398 nm on a Synergy4 Hybrid Multi-Mode micro plate reader (BioTek Inc, VT USA).[34] The culture supernatants were assayed after incubation with 1 mM Na EDTA for 12 h. The EDTA was added to remove chelated metal from the siderophore.[24,34]

2.6. Statistical analyses

For statistical analysis of cell density and phenazine accumulation, data from all of the three individual experiments were incorporated as independent replicates; the duplicate samples within each experiment being considered to be subsamples.

The effect of treatment of NPs/ions on colony count, or the accumulation of phenazines in the culture medium and in the pellets was assessed using a general linear mixed model. Treatment was a fixed effects factor. The design structure was a randomized block design with subsamples; experiment and the interaction of experiment and treatment were random effects factors. The mean of each treatment level was compared to the mean of the control level using Dunnett's method. Absorbance (366 nm) values were square-root transformed prior to analysis to better meet assumptions of normality and homogeneity of variance. Estimates of means and standard errors are re-transformed to the original scale for presentation in tables and figures. Data analyses were computed using the GLIMMIX procedure in SAS/STAT version 14.3 in the SAS System for Windows release 9.4 (TS1M3).

3 Results and discussion

3.1. Effects of ZnO NPs, Zn ions and cell growth on soluble levels of Zn in Phz medium

Soluble Zn in the Phz medium showed an initial value of 0.6 mg/L Zn which decreased to 0.1 mg/L after 48 h growth of *Pc*O6 cells (Table 1). We speculate that the decrease in soluble Zn seen with cell growth was due to utilization of Zn by the growing cells and binding of any Zn ions to cell components especially those in the bacterial cell wall.[36] Soluble Zn was released from NPs into the growth medium with dose dependency and with higher levels when cells were cultured (Table 1). This release of soluble Zn occurred in the Phz medium where aggregation of the NPs was observed by dynamic light scattering (Fig. 1). Large aggregates that ranged in size with a mean diameter of nearly 2000 nm were observed from the Phz medium suspension. Aggregation into a range of particle size also occurred in water suspension although the mean was of smaller size, 500 nm (Fig. 1). This difference may be due to associations of the NPs with materials in the medium as discussed below.

The addition of Zn ions to the medium resulted in a visible formation of a white precipitate with doses of 15 mg Zn ions/L and above. Analysis by ICP-MS of this precipitated material obtained from centrifugation of noninoculated Phz medium found the precipitate contained phosphate and Zn (data not shown) which agreed with the GEOCHEM prediction of the formation of insoluble Zn phosphate (Table 2). GEOCHEM analysis also showed that two amino acids in the medium, histidine and cysteine, would bind Zn as soluble complexes, and that the PIPES, present as a buffer in the medium, also bound Zn especially at the lower Zn concentrations. Only a small portion of soluble Zn was predicted to be as free ion (Table 2). The

closeness of the values measured in noninoculated medium amended with Zn ions and the predicted values (Tables 1 and 2) indicated that the major chelating compounds had been identified.

3.2. Examination of the interactions between ZnO NPs and *Pc*O6 cells in medium

Imaging of *Pc*O6 cells treated with the ZnO NPs was performed by confocal and HIM microscopy. Fig.2 A shows that the autofluorescent *Pc*O6 cells are associated with the grey-coloured aggregates of ZnO NPs that have formed in the Phz medium. The identity of the aggregates as being composed of ZnO NPs was determined by using high intensity excitation and noting the characteristic blue fluorescence of the structures. Fig. 2 B is a HIM image of the agglomerates of NPs on the smooth surface of the bacterial cells (indicated by arrows). Individual ZnO NPs of diverse shapes are visible. However aggregation of the NPs was observed. Such imaging indicated that aggregated NPs were in close association with the bacterial cell surface facilitating interaction with NPs or released metal.

3.3. Inhibition of phenazine production in *Pc*O6 cells by ZnO NPs and Zn ions

Addition of ZnO NPs to Phz medium changed pigmentation of 48 h cultures from the bright orange typical of the hydroxyphenazine products observed with nonamended cultures (Fig. 3). With 500 mg Zn from ZnO NPs/L only fluorescent yellow coloration was observed, typical of the fluorescent pyoverdine like siderophore (PVD) produced by *Pc*O6.[34] The cell densities determined in the 48 h - stationary phase cultures showed a statistical difference ($P<0.05$) from the control values only for the treatment with 500 mg Zn/L. However all cultures were above 10^9 cells/ml, characteristic of stationary phase. Measurement of pH of the cultures showed altered

pH was not a contributing factor to changes in metabolism, NP dissolution or speciation of released Zn (Table 3).

Colorimetric analysis of phenazines in extracts from the culture medium and cells showed that the levels decreased with increasing doses of ZnO NPs (Fig. 3). The changes in the secreted levels were significant at $P < 0.001$ for each of the treatments with ZnO NPs compared with the controls. For phenazine levels within the cells, all treatments with the ZnO NPs showed significant differences from the control at P values less than 0.05. Because the ZnO NPs reduced both the intracellular and secreted phenazine levels with a strong dose effect, the decreases in secreted phenazines were unlikely due to impaired transport. Inhibition was observed with 5 mg/L Zn from the NPs (65 % inhibition for the secreted product and 48 % for the intracellular phenazines) with increased inhibition to over 90 % at 500 mg/L.

Addition of Zn ions to the Phz medium also reduced orange pigmentation of the cultures (Fig. 3) and extraction from the culture medium and from the cell pellets showed reduced levels of phenazines that were statistically different from the controls at P values less than 0.05. (Fig. 3). However, there was no dose effect with the Zn ion treatments (Fig. 3). The reductions in the levels of secreted phenazines for 5 to 90 mg/L Zn ion treatments were similar to the reductions achieved by addition of 5 mg/L Zn as ZnO NPs (Fig.3). We observed in these studies that the acidification of the ethyl acetate extracts caused the orange pigmentation of the hydroxyphenazines to change to yellow (data not shown), as previously recorded.[37] However, this change in pigmentation was reversible upon neutralization of the extract and, thus, changes in $A_{366\ nm}$ were not due to decomposition of the 2- hydroxyphenazine.

Separation of the phenazines by chromatography and EIS identification enabled comparison of how the ZnO NPs or ions affected levels of two major phenazines, PCA and

2 OH-PCA (Fig. 4). Production of PCA was higher than the production of 2 OH-PCA. The 500 mg/L NP doses almost completely eliminated phenazine production (Fig. 4). However, the PCA level was more sensitive to Zn, added either as NPs or ions, than that of the 2 OH-PCA (Fig. 4). The identification of the 2 OH-PCA indicated that hydroxylation by the aromatic monooxygenase, PhzO,38 was not Zn sensitive.

3.4. Zn effects on AHSL production

Bioassay using the *C. violaceum* detector for the levels of AHSLs secreted by *Pc*O6 showed that both ZnO NPs and Zn ions affected their secretion (Fig 5 A); this sensor preferentially detected AHSLs with straight chain fatty acids.[22] Effects were dose-dependent although the ion treatments did not achieve the same level of reduction as the NPs (Fig. 5 A). AHSL signaling is required for phenazine production. One possibility for the decrease in phenazine levels stemmed from a study showing Zn ions to inhibit PhzE, the first enzyme in the pathway for phenazine biosynthesis [39] This enzyme when purified from a *Burkholderia* strain contained Zn in the active site and inhibition by Zn ions was shown *in vitro*.[39] In contrast the PhzE enzyme from *P. aeruginosa* had Mg, Co or Mn as functional cofactors.[40] A role for Zn, as a functional cofactor or an inhibitor for the enzyme from *P. aeruginosa* was not reported.[40] Like these phenazine-producing isolates, the *Pc*O6 genome also contained an homolog of *phzE* that is expressed during cell growth when phenazines are produced (Anderson, data not shown). Metal cofactors or inhibitors for PhzE produced by *Pc*O6 have not been studied. However, because Zn levels are predicted to be at the femtomolar concentration of Zn ions within the bacterial cell's cytoplasm[41]we speculate Zn inhibition of PhzE was unlikely to occur within the living cell.

Our studies did support that changes in production of cell signaling compounds, AHSLs, were involved in regulating phenazine formation occurred in cells exposed to Zn. Chromatographic separation and analysis of the AHSLs showed that the extracts from culture medium without Zn additions contained 3-OH C6 and 3-OH C8 AHSLs as the major secreted products; this identification of C4 and C6 AHSLs confirmed the positive responses with the biosensor assay (Fig. 5B). Amendments of the medium with ZnO NPs and Zn ions caused dose-dependent declines in secreted AHSLs (Fig. 5C). A low level of 3-OH C6 AHSL was detected in extracts from the cells when exposed to the 500 mg/L NP dose. The Zn ion treatments also reduced the level of the major AHSL in extracts from the cell pellets (Fig. 5D). The decreases in both the secreted and the cellular accumulations of AHSLs indicated that Zn was unlikely to be impairing the AHSL secretion process.

The ZnO NPs were more effective in reducing AHSL and phenazine synthesis than Zn ions even when the levels of soluble Zn detected in the medium were similar, e.g. 8-9 mg/L, from additions of 50 mg/L ZnO NPs and 15 or 30 mg/L Zn ions. GEOCHEM modelling predicted that the free Zn ion levels in the medium would be very low. However, we speculate that surface to surface interactions between ZnO NPs with the bacterial cells would generate localized metal release such that the levels available to the cell were not duplicated by addition of ions to the medium. Similarly, associations of Ag NPs with the outer structures of another Gram-negative bacterium, *Escherichia coli*, also were viewed as being important in enhancing the toxicity of the NPs versus Ag ions. [42,43]

These findings with ZnO NPs extend the concern of sublethal levels of NPs changing quorum sensing systems in bacteria. Recently modifications in AHSL production were reported for *P. syringae* when exposed to Ag and carbon nanotubes.[44] Previous work had suggested that

AgCl-TiO_2 NPs could be added to materials used for food packing because of their suppression of AHSL production in *C. violacearum*.[45] Thus this phenomenon of aggravation of bacterial intercellular communication by NPs could be widespread.

3.5. Role of Fe in altered production of phenazines and PVD

The NPs did not contribute soluble Fe to the culture medium (Table 1). The level of soluble Fe was reduced by cell growth, but remained at a similar level with all Zn amendments (Table 1), perhaps due to chelation of Fe with the PVD siderophore. Without cells, soluble Fe decreased with increasing Zn, indicating possible interactions as phosphate complexes (Table 1).

The amendment of the Phz medium with ZnO NPs resulted in dose-dependent increase in production of a fluorescent PVD-like siderophore (Fig. 6), confirming previous findings where a Fe-deficient medium supporting *Pc*O6 growth was amended with 500 mg Zn/L from ZnO NPs.[34] The level of PVD-related fluorescence markedly increased when cultures were supplemented with 50 and 500 mg/L NPs or 30 and 90 mg/L Zn ions (Fig. 6). Fluorescence in the Zn-amended culture filtrates, when excited at 398 nm, had a broad peak at 500 nm. However, addition of 1 mM EDTA, to remove all chelated metals, shifted emission to between 460 and 465 nm, indicative of the PVD lacking metal chelation. These findings were consistent with the formation of a Zn-PVD complex with a skewed fluorescence peak.

Growth of *Pc*O6 in Phz medium amended with 5.6 mg/L (100 μM) Fe reduced fluorescence of the culture filtrates when compared to the value of the control cultures (e.g. for the culture with no Zn addition relative fluorescent units (RFU) were 1630 ± 380, compared with culture with Fe addition, RFU 280 ± 100). This reduction in fluorescence was as expected due integration of Fe into the PVD structure to generate a nonfluorescent product.[34] However, the

addition of Fe also increased both PCA and 2-OH PCA for the secreted and cell-bound products (Fig. 7). These findings suggest an inverse relationship between Fe and phenazines, with Fe stimulating phenazine production but repressing PVD formation. An increase in phenazine production with Fe previously was reported for *P. chlororaphis* PCL1391, when effects on phenazine-1-carboxamide were examined.[46, 47] It is possible that phenazine reduction in the *Pc*O6 cells exposed to Zn could be attributed to lack of Fe in the cell. It is interesting that phenazines are thought to be important in Fe acquisition for pseudomonads. Phenazines produced by *P. aeruginosa* caused reduction of ferric to ferrous minerals, with resultant increased bioavailability to the cell because of Fe^{2+} uptake.[48, 49] This process was sensitive to oxygen levels and, thus, its significance to our shake culture assay conditions is uncertain. Also the phenazine 1- hydroxyphenazine acts as a Fe chelator of sufficient strength to contribute to fungal antagonism[14]; whether the phenazines produced by *Pc*O6 also chelate Fe is not known.

The phenotypes of lowered AHSLs and, thus, phenazine production but increased siderophore secretion are similar to those of a *Pc*O6 *gacS* mutant which was impaired in phenazine and AHSL formation but overproduced PVD.[7, 30] The mechanism underlying this process may relate to the need of the cell to limit Fe because of its connections to reactive oxygen stress. The *gacS* mutant has a reduced complement of enzymes, such as catalase/peroxidase isozymes, resulting in increased sensitivity to oxidative stress.[50] However, there also may be lowering of Fe availability in the *Pc*O6 cells exposed to ZnO NPs because of competition between Fe and Zn for cellular uptake. The reduced availability of Fe would then induce PVD synthesis. Induction of fluorescent siderophore synthesis by Zn ions was documented previously for *P. fluorescens*[51], and *P. aeruginosa.*[52] It is speculated[52] that Zn ions altered Fe uptake into the cell in part because Zn-chelated PVD inhibited unloading of FePVD

leading to yet further increases in production of PVD. Similarly Zn was proposed to compete in uptake with Fe in *Azotobacter vinelandii.*[53,54] Changes in metal uptake may also relate to interaction between Zn ions and the regulator Fur that normally represses genes involved in siderophore synthesis.[54] Additionally the reduction in level of the phenazines may be involved in the changes in siderophore production. The phenazine, pyocyanin, has been proposed to act as a cell signal regulator in *P. aeruginosa* with observed down-regulation of genes encoding proteins involved in Fe^{3+} uptake, as well as in Zn transport, *znuA* and *znuC,* and the regulator of this uptake system, *np20*[31] Further connection between Zn metabolism and phenazine formation in *P. aeruginosa* is suggested from the fact that a mutation in *np20* resulted in eliminating pyocyanin formation.[56] Whether these Fe-Zn interactions relate to the Gac sensor kinase requires additional studies.

Although the mechanism underlying the Zn effects on AHSL and siderophore production requires clarification, there is evidence of this process occurring in the rhizosphere. In studies with bean, *Pc*O6 colonization resulted in increased siderophore levels being detected in the rhizosphere solution upon growth in the presence of Zn ions or ZnO NPs.[57]

4 Conclusions

We found that *Pc*O6 responded to sublethal levels of ZnO NPs by changes in metabolites involved in intracellular and interspecies cell signaling. Reduction in phenazine production was observed with low doses of Zn (5 mg/L) from ZnO NPs when the extent of the response was nanoparticle-specific. Induction of siderophores involved higher Zn exposure levels. Changes in phenazines corresponded with inhibition of the AHSL-quorum sensing mechanism which for the

root colonizing bacterium, *Pc*O6 , could have serious consequences in the rhizosphere. The AHSL-quorum sensing system system in *Pc*O6 controls many traits associated with its survival plus stress responses in plants. These findings suggest that ZnO NP presence in the agricultural environment has the potential to complicate the effects of beneficial rhizobacteria on plant performance.

Acknowledgements

We are grateful for the support of the United States Department of Agriculture (USDA-CSREES) grant 2011-03581, the Utah Agricultural Experiment Station, and the Utah Water Research Laboratory. Utah Agricultural Experiment Station (Journal Paper 8887). We thank Susan Durham for the statistical analysis.

References

1 M.J. Osmond, and M.J. McCall, *Nanotoxicology*, 2010, **4**:15–41.

2 H. Zhang, B. Chen, H. Jiang, C. Wang, H. Wang, and X. Wang, *Biomaterials*, 2011, **32:**1906–1914.

3 M.E. Burnett, and S.Q.Wang, *Photodermatol. Photoimmunol. Photomed*, 2011, **27**:58–67.

4 J. Song, J. Zhou, and Z.L. Wang, *Nano Letters***, 6:**1656–1662

5 N. Milani , M.J. McLaughlin, S.P. Stacey, J.K. Kirby, G.M. Hettiarachchi, D.G. Beak, and G. Cornelis, *Agric. Food Chem.*, 2012, **60**:3991-3998.

6 A. Servin, W. Elmer, A. Mukherjee, R. de la Torre-Roche, H. Hamdi, J.C. White, P. Bindraban and C. Dimkpa. *J. Nanopart. Res.*, 2015, **17**: 92-

7 M. Spencer, C.M. Ryu, K.W. Yang, Y.C. Kim, J.W. Kloepper, and A.J. Anderson, *Physiol. Mol. Plant Pathol.*, 2003, **63**:27–34.

8 S.M. Cho, B.R. Kang, S.H. Han, A.J. Anderson, J.Y. Park, Y.H. Lee, B.H. Cho, K.Y. Yang, C.M. Ryu, and Y.C. Kim. *MPMI*, 2008, **21**:1067–1075.

9 S.A. Oh, J.S. Kim, S.H. Han, J.Y. Park, C. Dimkpa, C. Edlund, A.J. Anderson, and Y.C. Kim, *Can. J. Microbiol.,* 2013, **59:**556-562.

10 J.H. Lee, K.C. Ma, S.J. Ko, B.R. Kang, I.S. Kim, and Y.C. Kim, *Curr. Microbiol,* 2011, **62**:746-751.

11T. Fang, J.L. Watson, J. Goodman, C.O. Dimkpa, N. Martineau, S. Das, J. E. McLean, D.W. Britt, and A.J. Anderson, *Microbiol. Res*., 2012, 91-98.

12 H.B. Krishnan, B.R. Kang, H.A. Krishnan, K.Y. Kim, and Y.C. Kim, *Appl. Environ. Microbiol*., 2007, **73**:327–330.

13 D.V. Mavrodi, O.V. Mavrodi, J.A. Parejko, R.F. Bonsall, Y.S. Kwak, T.C. Paulitz, L.S. Thomashow, and D.M. Weller, *Appl. Environ. Microbiol.*, 2012, **78**:804–812.

14 B. Briard, P. Bomme, B.E. Lechner, G.L. Mislin, V. Lair, M.C. Prévost, J.P. Latgé, H. Haas, and A. Beauvais, *Sci. Rep.,* 2015, **5**:8220.

15 F.E. Olorunleke, G.K. Hua, N.P. Kieu, Z. Ma, and M. Hofte, *Environ. Microbiol. Rep.,* 2015, **7**:774-781.

16 B.R. Kang, S.H. Han, R.E. Zdor, A.J. Anderson, M. Spencer, K.Y. Yang, Y.H. Kim, M.C.Y. Lee, B. H. Cho, and Y.C. Kim, *J. Microbiol. Biotechnol.,* 2007, **17**:586-593.

17 C. Selin, R. Habibian, N. Poritsanos, S.N. Athukorala, D. Fernando, and T.R. de Kievit**,** *FEMS Microbiol. Ecol.,* 2010, **71**:73-83.

18 Y. Wang, S.E. Kern, and D.K. Newman, *J. Bacteriol*., 2010, **192**:365-369.

19 L.E. Dietrich, T.K. Teal, A. Price-Whelan, and D.K. Newman, *Science*., 2008, **321:**1203-1206.

20 T. Das, and M. Manefield, *PLoS One.*, 2012, **7**:e46718.

21 D. Wang, J.M. Yu, R.J. Dorosk, L.S. Pierson, and E.A. Pierson, *PLoS One.,* 2016, **11**:e0148003.

22 S.R. Khan, J. Herman, J. Krank, N.J. Serkova, M.E. Churchill, H. Suga, and S.K. Farrand, *Appl. Environ. Microbiol.,* 2007, **73:**7443-7455.

23 J.E. Loper, K.A. Hassan, D.V. Mavrodi, E.W. Davis II, C.K. Lim, B.T. Shaffer, L.D. Elbourne, V.O. Stockwell, S.L. Hartney, *et al.*, *PLoS Genet.,* 2012, **8**:e1002784.

24 C.O. Dimkpa, A. Calder, J.E. McLean, D.W. Britt, and A.J. Anderson, *Environ. Pollut.,* 2011, **59**:1749-1756.

25 C.O. Dimkpa, J.E. McLean, E. Drew, E. Latta, E. Manago. D.W. Britt, W.P. Johnson, M.I. Boyanov, and A.J. Anderson, *J. Nanopart. Res.,* 2012, **14**:1125.

26 P.J. Slininger, and M.A. Jackson, *Appl. Microbiol. Biotechnol.,* 1992, **37:** 388-392.

27 P. Gajjar, B. Pettee, D.W. Britt, W. Huang, P.W. Johnson, and A.J. Anderson, *J. Biol. Eng.,* 2009, **3**:9.

28 D.R. Parker, W.A. Norvell, R.L. Chaney, R.H. Loeppert, A.P. Schwab, and S. Goldber (*eds*.), *Soil Sci. Soc. of Am.,* 1995, **42**: 253–269.

29 L. Housley, T. Anderson, N. Sontag, S.H. Han, D.W. Britt, and A.J. Anderson, F*EMS Microbiol. Lett.,* 2009, **293**:148–153.

30 S.A. Oh, J.S. Kim, J.Y. Park, S.H. Han, C. Dimkpa, A.J. Anderson, and Y.C. Kim. *Plant Pathol. J*., 2013, **29**:323-329.

31 L.E. Dietrich, A. Price-Whelan, M. Whiteley and D.K. Newman, *Mol. Microbiol.,* 2006, **61**:1308-1321.

32 C. Cha, P. Gao, Y.C. Chen, P.D. Shaw, and S.K. Farrand, *Mol. Plant-Microbe Interact.,*1998, **11:**1119-1129.

33 C.O. Dimkpa, J.E. McLean, D.W. Britt, W.P. Johnson, B. Arey, S.A. Lea, and A.J. Anderson, *Chem. Res. Toxicol.,* 2012, **25**:1066-1074.

34 C.O. Dimkpa, J.E. McLean, D.W. Britt, and A.J. Anderson, *Nanotoxicology,* 2012, **6**: 635-642.

35 S.A. Oh, J.S. Kim, S.H. Han, J.Y. Park, C. Dimkpa, C. Edlund, A.J. Anderson, and Y.C. Kim, *Can. J. Microbiology*., 2013, **59**:556-562.

36 J.E. McLean, M.W. Pabst, C.D. Miller, C.O. Dimkpa, and A.J. Anderson, *Chemosphere*, 2013, **91:**374-382.

37 J.I. Toohey, D. Nelson, and G. Krotko, *Can. J. Bot.,* 1965, **43**:1055-1102.

38 S. M. Delaney, D.V. Mavrodi, R.F. Bonsall, and L.S. Thomashow, *J. Bacteriol.,* 2001, **183**:318-327.

39 Q.A. Li, D.V. Mavrodi, L.S. Thomashow, M. Roessle, and W. Blankenfeldt, 2011, *J.Biol. Chem*., **6:**18213-18221.

40 J.E. Culbertson, and M.D. Toney, *Biochim. Biophys Acta*., 2013, **1**:240-246.

41 C.E. Outten, and T.V. O'Halloran**,** *Science,* 2001, **292**: 2488-2492.

42 J.S. McQuillan and A.M. Shaw, *Nanotoxicology*, 2014, **8:**177–184.

43 J.S. McQuillan, H.G. Infante, E. Stokes, and A.M. Shaw, *Nanotoxicology*, 2012, **6**:857–866.

44 A.N. Mohanty, C.H. Tan, and B. Cao, *Environ. Sci. Nano*, 2016, **3**, 351-356.

45 K. Naik, and M. Kowshik, *J. Appl. Microbiol.* 2014, **117:**972-983.

46 E.T. van Rij, G. Girard, B.J. Lugtenberg, and G.V. Bloemberg, *Microbiology*, 2005, **151**:2805-2814.

47 E.T. van Rij, W. Wesselink, T.F. Chin-A-Woeng, G.V. Bloemberg, and B.J. Lugtenberg, *Mol Plant Microbe Interact.*, 2004, **17**:557-566.

48 Y. Wang, and D.K. Newman, *Environ. Sci. Techno*l**.**, 2008**, 42**:2380-2386.

49 Y. Wang, J.C. Wilks, T. Danhorn, I. Ramos, L. Croal, and D.K. Newman, *J. Bacteriol.,* 2011, **193**:3606-3617.

50 B.R. Kang, B.H. Cho, A.J. Anderson, and Y.C. Kim, *Gene.*, 2004, **325**:137-143.

51 S. Rossbach, T.L. Wilson, M.L. Kukuk, and H.A. Carty, *FEMS Microbiol. Lett.,* 2000, **191:**61-70.

52 M. Hofte, S. Buysens, N. Koedam and P. Cornelis, *Biometals.*, 1993, **6:**85–91.

53 M. Huyer, and W.J. Page. *Appl. Environ. Microbiol*., 1988, **54**:2625-2631.

54 M. Huyer, and W.J. Page, *J. Bacteriol*., 1989, **171**:4031–4037.

55 V. Hancock, M. Dahl, and P. Klemm, *Appl. Environ. Microbiol.,* 2010, **76:**3836–3841.

56 L.A. Gallagher, S.L. McKnight, M.S. Kuznetsova, E.C. Pesci, and C. Manoil. *J. Bacteriol*., 2002, **184**:6472-6478.

57 C.O. Dimkpa, T. Hansen, J. Stewart, J.E. McLean, D.W. Britt, and A.J. Anderson, *Nanotoxicology*, 2015, **9:**271-278.

Tables

Table 1 Concentrations of soluble Zn and Fe measured in Phz medium after 48 h with additions of ZnO NPs or Zn ions with or without growth of *Pc*O6 cells

Zn Concentration (mg/L)	Measured Soluble Fe (µg/L)		Measured Soluble Zn (mg/L)	
	With Cells	Without Cells	With Cells	Without Cells
0	10.9 ± 1.6 **a**	36.3 ± 4.4 **a**	0.1 ± 0.1 **a**	0.6 ± 0.1 **a**
ZnO NPs - 5	8.1 ± 0.0 **a**	32.2 ± 3.3 **ac**	2.3 ± 0.4 **a**	4.4± 0.1 **ab**
ZnO NPs - 50	7.4 ± 0.2 **a**	5.4 ± 0.0 **b**	11.8 ± 5.4 **b**	9.3 ± 3.5 **bc**
ZnO NPs - 500	8.3 ± 2.0 **a**	7.4 ± 0.1 **b**	25.7 ± 9.1 **c**	10.7 ± 5.9 **b**
Zn Ions - 5	9.8 ± 3.1 **a**	30.0 ± 2.6 **c**	1.7 ± 0.1 **a**	3.7 ± 0.4 **ac**
Zn Ions - 15	8.2 ± 1.1 **a**	6.7 ± 1.7 **b**	4.7 ± 0.1 **ab**	8.2 ± 0.6 **bc**
Zn Ions - 30	11.6 ± 5.7 **a**	7.9 ± 4.8 **b**	7.7 ± 0.3 **ab**	8.9 ± 0.2 **bc**
Zn Ions - 90	14.9 ± 3.5 **a**	3.0 ± 0.5 **b**	27.3 ± 3.8 **c**	19.4 ± 3.8 **d**

Data are from two independent studies each with two replicates; mean and standard error are shown.

Numbers followed by different letters are statistically different at p=0.05.

Table 2 Predictions based on GEOCHEM modeling at pH 6.8 of the speciation of Zn in the Phz medium when added at 5, 30 and 90 mg/L.

Form	**5 mg Zn/L**	**30 mg Zn/L**	**90 mg Zn/L**
Free ion	4.45 %	1.68 %	0.66 %
cysteine	38.25 %	11.26 %	4.30 %
PIPES	51.99 %	19.25 %	9.27 %
histidine	2.45 %	0.84 %	0.33 %
PO4 (soluble)	0.87 %	0.29 %	0.09 %
PO4 (insoluble)	0.00 %	65.97 %	85.04 %
Calculated soluble Zn (mg/L)	**5**	**10.2**	**13.5**
***Measured soluble Zn (mg/L)**	**3.7**	**8.9**	**19.4**

*The measured values were from data shown in Table 1.

Table 3 Effect of the presence ZnO NPs or Zn ions on growth of *Pc*O6 for 48 h: pH of the culture filtrate and cell density (colony forming units CFU/ml)

***Pc*O6/Zn Cultures (mg/L)**	**Culture Filtrate pH**	**CFU/ml ($x10^9$)**
0	6.77 ± 0.03	6.0 ± 1.4
NPs ZnO - 5	6.78 ± 0.00	5.1 ± 1.5 (P=0.8)
NPs ZnO - 50	6.80 ± 0.02	4.2 ± 01.4 (P=0.2)
NPs ZnO - 500	6.79 ± 0.02	2.8 ± 0.9 (P=0.04)
Ions - 5	6.78 ± 0.01	6.7 ± 1.2 (P= 0.8)
Ions - 15	6.77 ± 0.04	7.3 ± 0.6 (P=0.5)
Ions - 30	6.78 ± 0.01	5.0 ± 1.0 (P=0.5)
Ions - 90	6.73 ± 0.00	5.7 ± 1.5 (P=0.6)

The pH data are from one experiment with two replicates for each treatment. The cell numbers are means of three independent experiment each with two replicates for the ZnO NPs and ion treatments. . Dunnetts method was used to determine P - value for comparisons to the control means after an omnibus test showed an overall treatment effect with a P - value of 0.077.

Figures

Fig. 1 Dynamic light scattering analysis of ZnO NPs (200 mg Z/L from the NPs) aggregation in Phz medium compared with water after suspension for 5 h. Data are means of ten five second acquisitions and are typical of three separate studies.

Fig. 2 Microscopic images showing association of ZnO NPs with *Pc*O6 cells.

Figure 2 A Images of a mixed suspension of cells with ZnO NPs by confocal microscopy taken 30 min after addition of 500 mg Zn/L from ZnO NPs with cells in medium. Excitation was at 405 nm and the autofluorescence of the bacterial cells was recorded by collecting fluorescence in the blue (410-495 mm), green 495-581 nm and red 584-735 nm) fluorescence. The arrows note the association of the agglomerates of ZnO NPs with the fluorescent bacterial cells. The inset shows the agglomerates have the typical blue fluorescence characteristic of ZnO NPs when excited with at higher power and showing emission only between 410-495 nm.

Fig. 2 B HIM imaging of *Pc*O6 cells after culture in Phz medium with ZnO NPs. The arrows indicate the smooth bacterial cell surface underlying the NP overlay. Aggregates of ZnO NPs with dimensions less than 100 nm are visible associated with the cell surface.

Fig. 3 Effects of amendments of Phz medium with ZnO NPs or with Zn ions on phenazine production by *Pc*O6. Pigmentation in cultures after 48 h growth with and without amendments of ZnO NPs (5, 50 and 500 mg Zn/L) or 5, 15, 50 and 90 mg/L Zn ions from $Zn(NO_3)_2$ is shown. The soluble Zn (mg/L) measured

in the medium with and without amendments of Zn from NPS or ions is provided using data from Table 1. The levels of phenazine, either as secreted products or associated with the cell (cellular product), as determined in extracts by measurement of absorbance at 366 nm are shown. The data are the means of three separate experiments each of which had two replicate cultures for each treatment. Standard errors are provided. Statistical analysis by Dunnetts method showed P-values for comparison to control of <0.001 for the 5, 50 and 500 mg/L treatments with ZnO NPs and 0.013, 0.002 and <0.001 for the Zn ions at 5. A. 30. 60 and 100 mg/L respectively when secreted phenazines were measured. All the values for the phenazines in Zn-exposed cell extracts were statistically different from the controls at P <0.001 The * denotes statistical differences between values for treatments versus controls.

Fig.4 Effects of amendments of the medium with ZnO NPs and Zn ions on the composition of secreted phenazines. The data are from analysis of the chemicals PCA and 2 OH PCA based on mass spectral identification of peaks from HLPC separation with processing using the Agilent MassHunter Software. Data are means of two independent cultures from one study but are consistent with a second separate study.

Fig. 5 Effects of ZnO NPs and Zn ions on the level and composition of AHSLs. (A) Levels of AHLS as detected by the biosensor, *C. violaceum,* using extracts of the culture medium from 48 cultures. (B). The array of AHSLs detected in culture medium of cells grown under control conditions in Phz medium for 48 h; (C) Composition of AHSLs secreted from *Pc*O6 when grown in Phz medium for 48 h cultures in the presence and absence of amendments of ZnO NPs and Zn ions. (D) Effects of ZnO NPs and Zn ion additions to Phz medium on accumulation of 3-OH C6 AHSL production within cells. Data are based on two replicated studies; mean and standard errors are shown.

Fig. 6 Effect of ZnO NPs and Zn ions on production of PVD-like siderophores from *Pc*O6. The fluorescence data, based on excitation at 398 nm and emission at 365 nm are from 48 h cell-free culture filtrates treated with 1 mM EDTA for 24 h; RFU relative fluorescence units. % values are related to control values

with no Zn additions. Cultures were prepared in the presence and absence of added ZnO NPs and Zn ions. Data are the means of two replicates/treatment from one study but are typical of three independent studies.

Fig.7 Effect of Fe on phenazine production in *Pc*O6 cultured in Phz medium for 48 h. Effect of Fe (5.6 mg/L) in the Phz medium on the levels of phenazines secreted into medium or associated with the pellet, (A) As assessed by $A366_{nm}$. The ethanol extracts were diluted x100 fold to generate these data. (B) Altered production of PCA and 2 OH-PCA as determined by HPLC MS EIS analysis of the ethanol solutions obtained from acidified ethyl acetate extracts. Data are averages and standard errors of two separate studies.

Figure 1

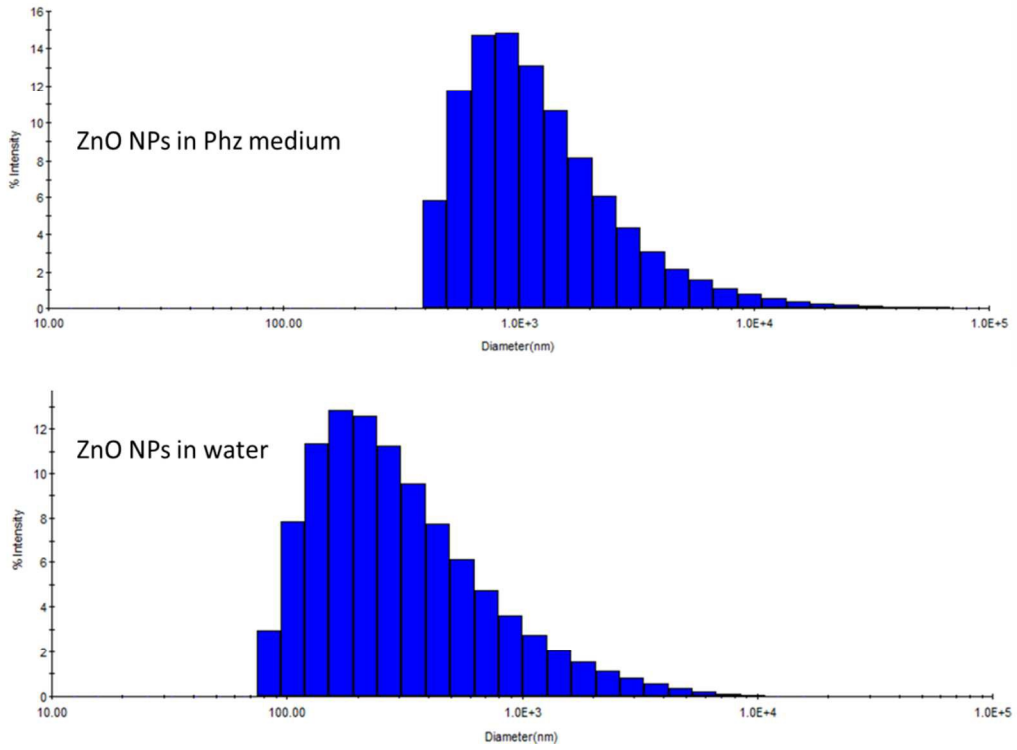

Figure 2.

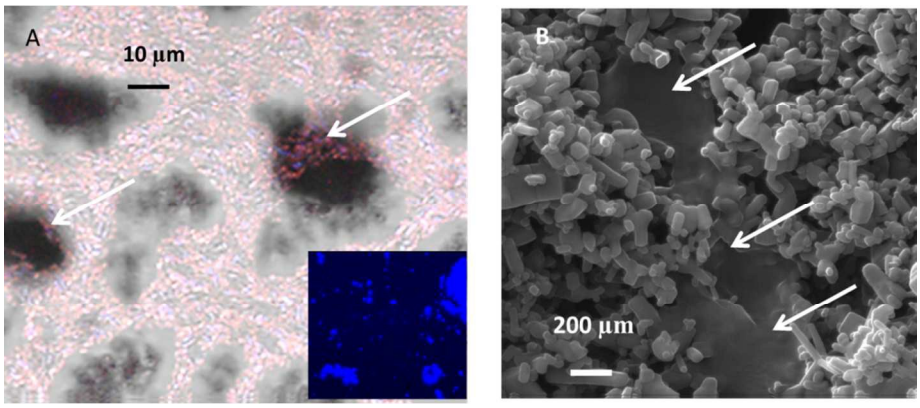

Figure 3

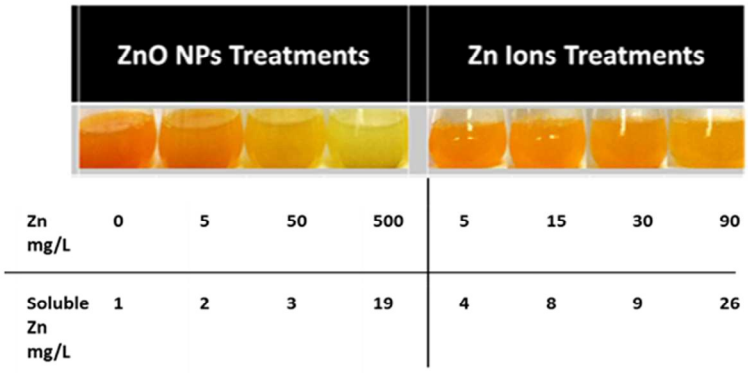

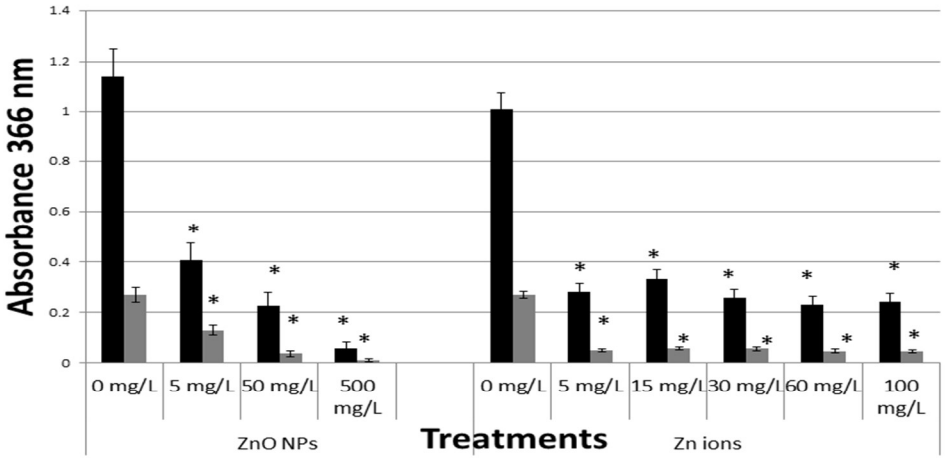

Figure 4

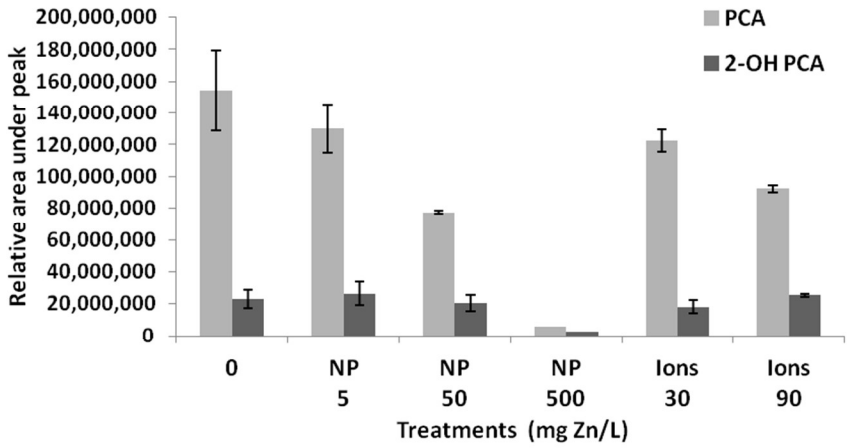

Figure 5

A. Relative levels of secreted AHSLs detected with the biosensor *C. violaceum*

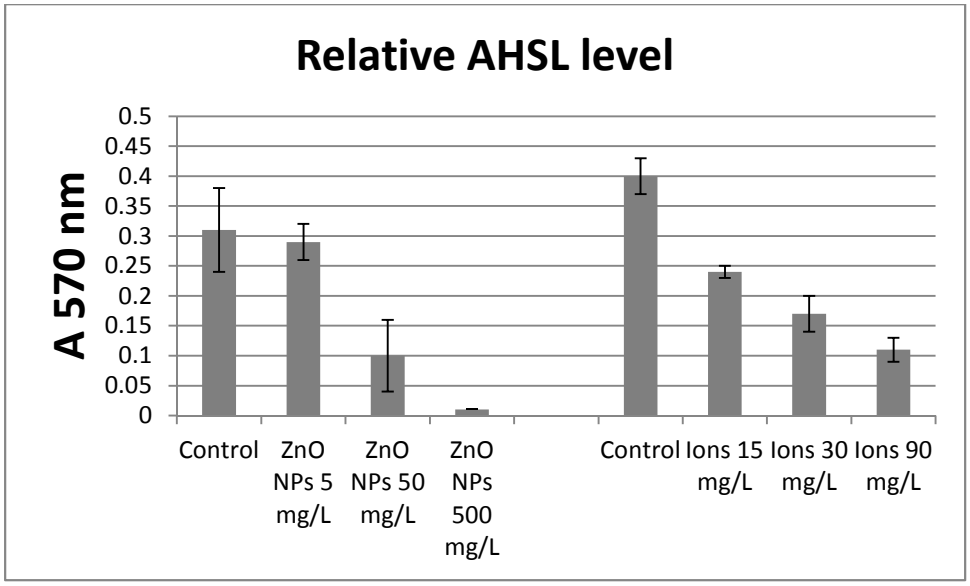

B Array of secreted AHSLs detected in *Pc*O6 grown in cultures lacking Zn amendments

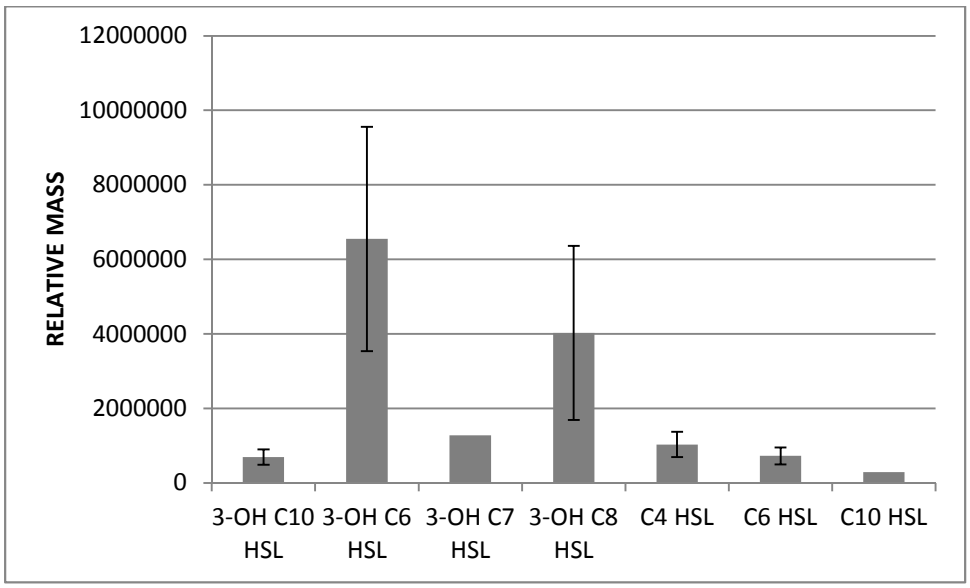

C. Effects of ZnO NPs and ions on the major secreted AHSLs

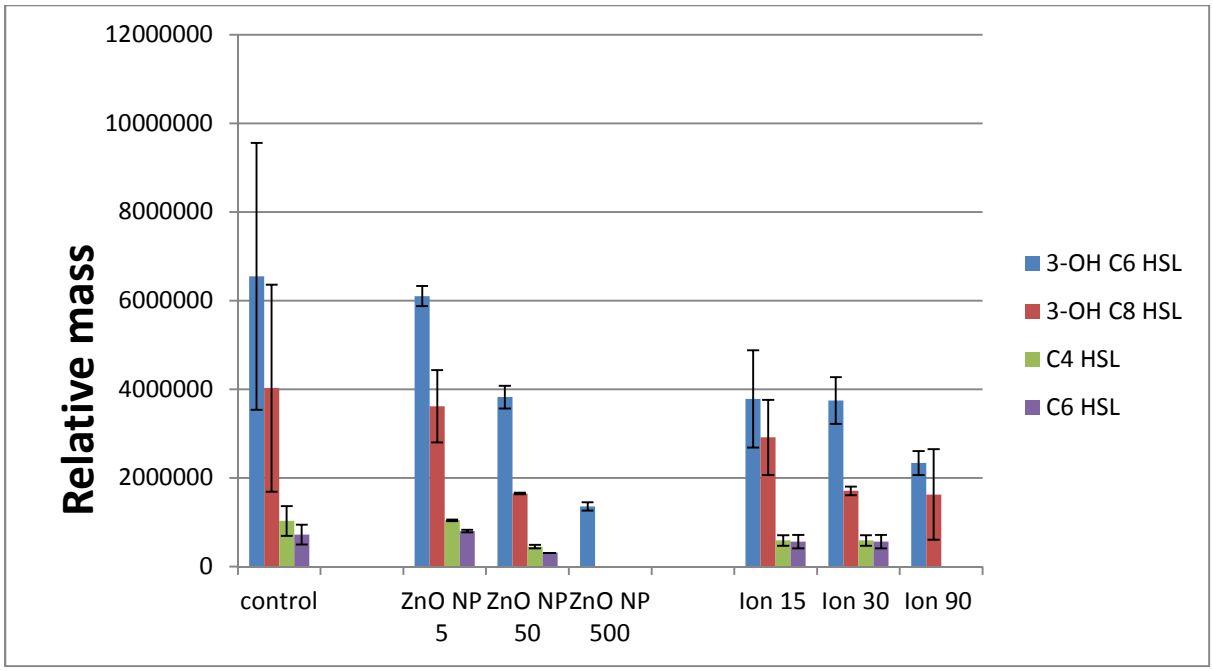

D. Effects of ZnO NPs and Zn ions on the major AHSL, 3-OH C6 AHSL, in cell pellets

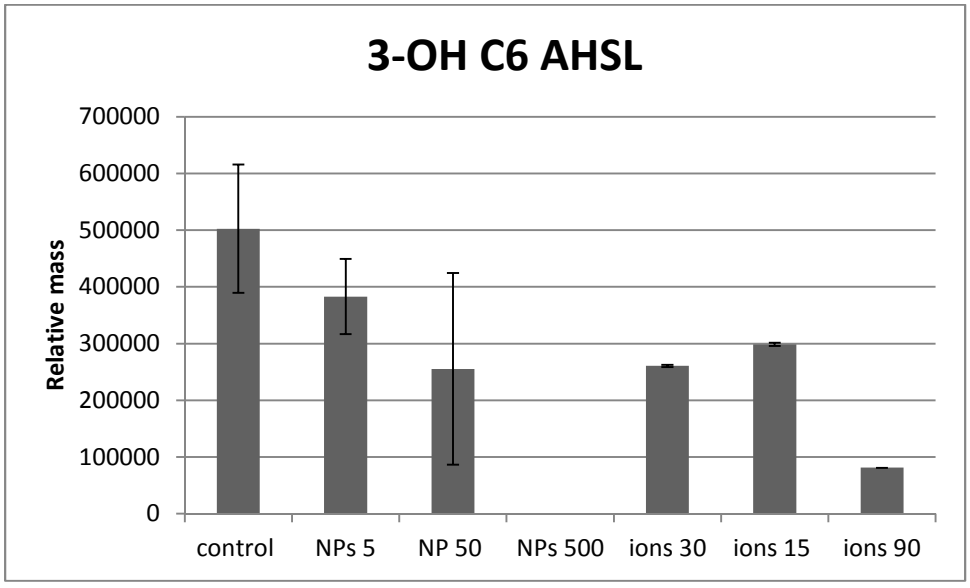

Figure 6.

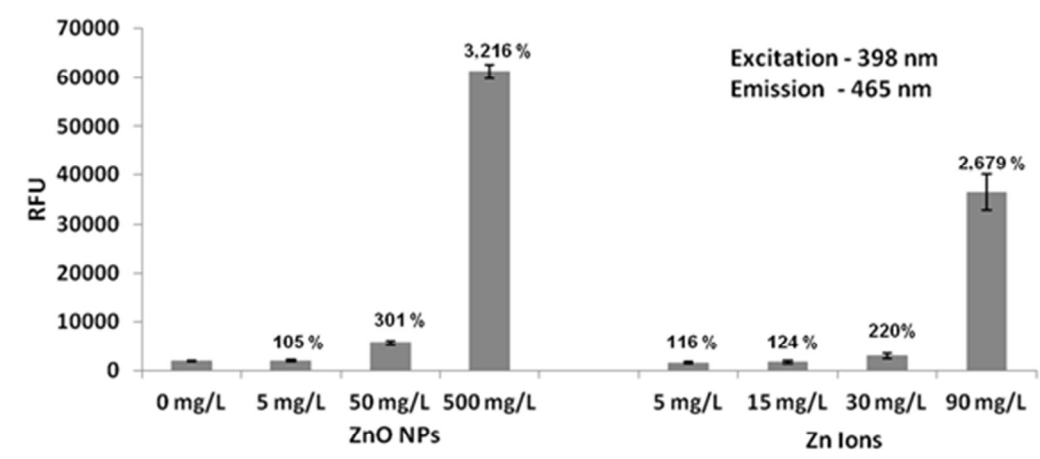

Figure 7.